Food Chemistry: X 19 (2023) 100792

Contents lists available at ScienceDirect

Food Chemistry: X

journal homepage: www.sciencedirect.com/journal/food-chemistry-x

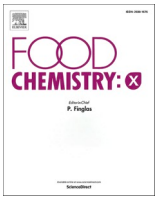

Analytical Methods

A smartphone-assisted colorimetric aptasensor based on aptamer and gold nanoparticles for visual, fast and sensitive detection of ZEN in maize

Liyuan Zhang [a,*], Jiayu Chen [a], Lifeng Lu [a,1], Runzhong Yu [b,*], Dongjie Zhang [a,c,d,*]

[a] College of Food Science, Heilongjiang Bayi Agricultural University, 5 Xinfeng Road, Daqing 163319, PR China
[b] College of Information and Electrical Engineering, Heilongjiang Bayi Agricultural University, 5 Xinfeng Road, Daqing 163319, PR China
[c] Chinese National Engineering Research Center, Daqing 163319, PR China
[d] Key Laboratory of Agro-products Processing and Quality Safety of Heilongjiang Province, Daqing 163319, PR China

ARTICLE INFO

Keywords:
Zearalenone
Aptamer
Gold nanoparticles
Colorimetric aptamer sensor
Measurement
Smartphone assisted

ABSTRACT

A simple, fast, low cost, sensitive, intuitive, visual, label-free, and smartphone-assisted aptamer sensor based on colorimetric assay for the measurement of zearalenone was constructed. The nucleic acid aptamer of zearalenone was used as the recognition element and gold nanoparticles were used as the indicator. Several factors that could influence sensitivity, including the concentration of aptamer and NaCl, and incubation time, and specificity, have been investigated. The results showed that under the optimal conditions, the signal had a good linear relationship when zearalenone concentration is 5–300 ng/mL. A linear regression equation is $Y = 0.0003X + 0.5128$ ($R^2 = 0.9989$) and a limit of detection is 5 ng/mL. The specificity of the sensor was good. Zearalenone in maize samples were successfully measured. The recoveries of Zearalenone are 81.3 %-96.4 %. The whole process takes only 15 min to complete. The smartphone assisted colorimetric aptamer sensor can be used for the detection of zearalenone in maize.

1. Introduction

Zearalenone (ZEN), also known as F-2 toxin. It is a secondary metabolite produced mainly by fungi such as *Fusarium* and *Fusarium yellow*. And it is widely distributed among maize, wheat, barley, sorghum, rye, and other cereals (Aiko & Meht, 2015; Mally, Solferizzo, & Degen, 2016). ZEN can damage the immune, nervous, and reproductive systems of humans, thus posing a serious threat to human health (Solís-Cruz et al., 2017). Therefore, the establishment of effective methods for the detection of ZEN in foods is essential to safeguard human health.

There are conventional methods for the measurement of Zen (Appel & Bosma, 2011; Ji et al., 2019; Ropejko & Twaruzek, 2021), such as enzyme-linked immunosorbent assays (Goud et al., 2018), electrochemical immunoassays (Fernandez, Arevalo, Granero, Robledo, Díaz Nieto, Riber, & Zon, 2017), fluorescent immunoassays (Sharma, Ragavan, Thakur, & Raghavarao, 2015), microchip-based experiments (Man, Liang, Li, & Pan, 2017), electromigration-based experiments (Li et al., 2012), surface plasmon resonance immunoassays (Meneely & Elliott, 2014), GC–MS (Blokland et al., 2006), LC-MS (Kovalsky et al., 2016; Malachová, Stránská, & Václavíková, 2018; Zhao et al., 2021). However, these immunoassays are heavily dependent on the utilization of antibodies. In contrast, the preparation of antibodies by animal immunization is usually time-consuming, expensive. In addition, the kits are easily inactivated during storage and transportation and are not easily preserved. GC–MS and LC-MS requires tedious sample pretreatment, sophisticated instrumentation and skilled professionals.

A nucleic acid aptamer (aptamer) is a single-stranded oligonucleotide (ssDNA or ssRNA) sequence with high affinity that binds specifically to a target molecule. Due to its advantages of simple in vitro synthesis, high specificity, easy preservation and modification, low cost and high stability. Aptamers are considered to be the most promising alternatives to antibodies (Nimjee, Rusconi, & Sullenger, 2005). And based on the uniqueness of the aptamer, they can be combined with a wide range of technologies. They have been widely used in targeted therapies, disease detection, food safety testing and biomedical (Liu, Liu, Wang, Duan, & Yin, 2016). Sensors developed using aptamers as recognition elements have the advantages of high sensitivity, strong specificity, short detection time, and in situ detection. Therefore such sensors are increasingly favored by researchers (Chauhan, Singh, Sachdev, Basu, & Malhotra, 2016; Liu, Zhou, & Shi, 2015; Vasilescu & Marty, 2017; Wu et al.,

* Corresponding authors at: College of Food Science, Heilongjiang Bayi Agricultural University, 5 Xinfeng Road, Daqing 163319, PR China (D. Zhang).
E-mail addresses: zly1981_2005@163.com (L. Zhang), zly1981_2005@163.com (R. Yu), byndzdj@126.com (D. Zhang).
[1] Lifeng Lu and Liyuan Zhang are Co-first author.

https://doi.org/10.1016/j.fochx.2023.100792
Received 10 February 2023; Received in revised form 9 July 2023; Accepted 13 July 2023
Available online 18 July 2023

2018a). However, few researches have been reported on the development of smartphone assisted colorimetric aptasensor based on aptamers and gold nanoparticles (Goud et al., 2017; Taghdisi, Danesh, Ramezani, Sarreshtehdar, & Abnous, 2018). In recent years, aptamer based colorimetric sensing methods have been used due to their simplicity, low cost and high sensitivity. It has become an alternative method to detect various target molecules (Zhu et al., 2021). In this detection method, the aptamer is used as the recognition element, which helps to improve the specificity of the sensor (Nguyen & Jang, 2020). The gold nanoparticles (AuNPs) are widely used as colorimetric indicators due to their high color correspondence and controllable shape (Kafouris, Christofidou, Christodoulou, Christou, & Kakouri, 2017; Purohit, Vernekar, Shett, & Chandra, 2020; Zheng, Wang, & Yang, 2011).

In this work, a simple, rapid, visualized, label-free, and smartphone assisted color matching adapter sensor was constructed. The sensor used the adaptor as the recognition element and AuNPs as the indicator. ZEN could be sensitively detected by observing the color change of apatsensor. The key parameters and reliability of apatsensor were investigated through a series of experiments. The detection mechanism of ZEN in maize were explored.

2. Instruments, materials and methods

2.1. Instruments and equipment

VICTOR Nivo Multimode Microplate Reader (Perkin Elmer Enterprise Management Co., Ltd.), UV spectrophotometer (Han Yi Instruments Co., Ltd.), and JEM-2100F transmission electron microscope (Japan Electronics Co., Ltd.) were used. KQ-500DE ultrasonic cleaner (Kunshan Ultrasonic Instruments Co., Ltd.) and Vortex-Genie 2 vortex oscillator (Scientific Industries Co., Ltd.) were used. A 1260 series liquid chromatograph with fluorescence detector (Agient Technologies Co., Ltd.) and an Agilent Eclipse plus C18 column were used.

DFY-500 high-speed pulverizer (Zhejiang Yongkang Jinsui Machinery Manufacturing Co., Ltd.), TH2-82T water bath thermostatic oscillator (Changzhou Ronghua Instruments Co., Ltd.), and H2-16KR tabletop high-speed centrifuge (Hunan Kecheng Instruments & Equipment Co., Ltd.) were used.

2.2. Materials and reagents

Nucleic acid aptamer of Zearalenone (5′-GAT GGG GAA AGG GTC CCC CTG GGT TGG AGC ATC GGA CA-3′) (Chryseis, Anders, & Allen, 2011) was purchased from Sangong Bioengineering Co., LTD. The zearalenone (ZEN), aflatoxin B_1 (AFB_1), deoxynivalenol (DON), and T-2 toxin were from Bioengineering (Shanghai) Co. Ltd. ZEN enzyme-linked immunoassay kit was purchased from Shanghai Quicklings Biotechnology Co., Ltd. The sodium citrate, potassium dichromate, acetonitrile, and sodium chloride were purchased from Shanghai Maclean Biochemical Technology Co. The water used in the experiments were all ultrapure water (resistivity of 18.2 MΩ.cm). The organic solvents in the experiments were all chromatographic pure, and the other experimental solvents were analytical pure.

The maize was purchased in local supermarket (Daqing City, Heilongjiang Province, 12, 2021).

2.3. Experimental methods

2.3.1. Sample preparation

The maize samples were ground into powder by using pulverizer and sifted through 80 mesh screens. The spiked samples containing ZEN were prepared by spiking the ZEN standard solutions (10, 50, and 100 ng/mL) into samples. Each spiking level was analyzed in triplicate. A total of nine spiked samples were obtained for the three spiking levels.

To ensure a uniform distribution of ZEN, an appropriate amount of acetone was added to wet the sample powder. Then it was carefully stirred and dried at room temperature for 24 h before extraction. The spiked sample were kept in sealed bottles and stored.

According to GB5009.209–2016 GB5009-209 (2016) (Determination of zearalenone in food: liquid chromatographic method) the ZEN of maize samples were extracted. The 5 g of the spiked maize samples were added to a conical bottle containing 25 mL of extract solution (acetonitrile: water = 90:10). It was then shaken on a water bath thermostat at 45 ℃ for 1 h. The samples were filtered through 0.22 μm of PTFE filter membrane.

2.3.2. Preparation of AuNPs

The AuNPs was prepared by sodium citrate reduction method (Wu, Liu, Huang, & Wu, 2019). 100 mL of ultrapure water and 1 mL of 1% chloroauric acid solution were added into a 250 mL beaker pre-soaked with chromic acid washing solution. Then, the mixed solution was stirred and heated to boiling. 2.5 mL of 1% sodium citrate solution was added and stirred quickly for 10 min. After continuous stirring, the color of the solution changed from light yellow to black, then from black to purplish red, and finally from purplish red to burgundy. The solution was transparent. After the color stops changing, the solution was heated and stirred for 10 min, cooled to room temperature for preparation, and transferred to 4 ℃ for storage. The characteristic peaks, absorbance values and quality evaluation of the prepared AuNPs solutions were performed by UV spectrophotometry. The size, shape and homogeneity of AuNPs particles were also observed by transmission electron microscopy.

2.3.3. Optimization of NaCl concentration

For purpose of optimizing experiments and reducing errors, all experiments had to require in triplicate. Firstly, 100 uL of AuNPs solution was added to the wells of the microplates. Then 10 uL of different concentrations (0, 0.5, 1.0, 1.5, 2.0, 2.5, and 3.0 mol/L) of NaCl solution were mixed in the wells of the microplates, respectively. The color changes of solution were observed with the naked eye after the reaction at room temperature for 5 min. The absorbance values of AuNPs were measured to determine the degree of aggregation.

2.3.4. Optimization of ZEN aptamer concentration

For purpose of optimizing experiments and reducing errors, all experiments had to require in triplicate. Firstly, 100 uL AuNPs solution was added to the wells of the microplates. Then 10 uL ZEN aptamer solution with different concentrations (0, 1, 3, 4, 5, 7, and 9 μmol/L) were added to the wells of the microplates, respectively. All mixed solution were incubated for 5 min at room temperature. Then, 10 uL of NaCl solution (2 mol/L) were added to the mixed solution, respectively. The optimal concentration of aptamer was selected by adding 10 uL of NaCl solution to the reaction solution for 5 min at room temperature. The color changes of solution were observed by naked eye. The absorbance values were measured by a microplate reader.

2.3.5. Optimization of incubation time of AuNPs and aptamers

For purpose of optimizing experiments and reducing errors, all experiments had to require in triplicate. 100 uL of AuNPs solution and 10 uL of ZEN aptamer (5 umol/L) was added the wells of the microplates and incubated at room temperature for 5 min. Then, 10 uL of ZEN standard solution (30 ng/mL) was added and incubated at room temperature for 5 min. The 10 uL of NaCl solution (2 mol/L) was added and incubated for 0, 5, 10, 15, 20, 25, and 30 min, respectively. The absorbance values were measured with microplate reader.

2.3.6. Specificity detection of ZEN

For purpose of optimizing experiments and reducing errors, all experiments had to require in triplicate. 100 uL of AuNPs solution and ZEN aptamer solution at a concentration of 5 umol/L were added the wells of the microplates and incubated at room temperature for 5 min. Then, 10 uL of DON, ZEN, T-2, AFB_1 standard solution at concentration of 30 ng/

ml were added and incubated at room temperature for 5 min. 10 uL of NaCl solution (2 mol/L) was added and incubated at room temperature for 5 min. After incubation, the color changes were observed visually. The absorbance values were measured by microplate reader.

2.3.7. Analysis of actual samples

In order to explore the feasibility and practicability of the method, the ZEN of maize samples were detected and analyzed by the method established in this work. First, 100 uL of AuNPs solution and 10 uL of ZEN aptamer solution (5 umol/L) were added to the microplates and incubated at room temperature for 5 min. Then 10 uL of blank and spiked samples were added and incubated for 5 min. The 10 uL of NaCl solution (2 mol/L) was then added and incubated for 5 min. Finally, the absorbance values were measured with a microplate reader and the recoveries and RSD were calculated.

The differences between the method used in this work and the national standard method were also analyzed by T-Test. The Eclipse plus C18 column was 100 mm × 4.6 mm, 3.5 μm. The column temperature was 30.0 ℃, the column flow rate was 0.80 mL/min, and the injection volume was 10 μL. The excitation wavelength of the fluorescence detector was 274 nm and the emission wavelength was 440 nm.

2.3.8. Data processing software

The Origin 2021 was used for image production, IBM SPSS Statistics 25 was used for variance analysis. Thermo Scientific Velox software was used for acquisition of TEM image. Kaleido^{TM} data acquisition and analysis software was used for Victor Nivo multimode microplate reader.

3. Results and discussion

3.1. The measurement mechanism of the constructed sensor

The aggregation and dispersion states of AuNPs solution show different colors. Under normal conditions, citrate ions attached to the surface of AuNPs in the system can form an electrostatic protective layer, so that the AuNPs are evenly dispersed in the system to form a stable colloidal solution. But in high concentration of salt, AuNPs will aggregate and the color can change from wine red to blue. The aptamer was added to the solution, the AuNPs and the aptamer were bound by electrostatic adsorption, and the aptamer could protect the AuNPs from the induction of salt to maintain the dispersed state in the system, and the color of the system remains wine red. After added ZEN, the aptamer was detached from the surface of AuNPs and specifically bound to ZEN. The AuNPs lost protection of the aptamer and aggregated at high concentration of salt, and the color of the solution changed from red to blue. The degree of color change was positively correlated with the concentration of the added target ZEN. The detection mechanism is shown in Fig. 1. By characterizing the color change of AuNPs system, the visual, rapid qualitative and quantitative detection of ZEN in maize could be realized.

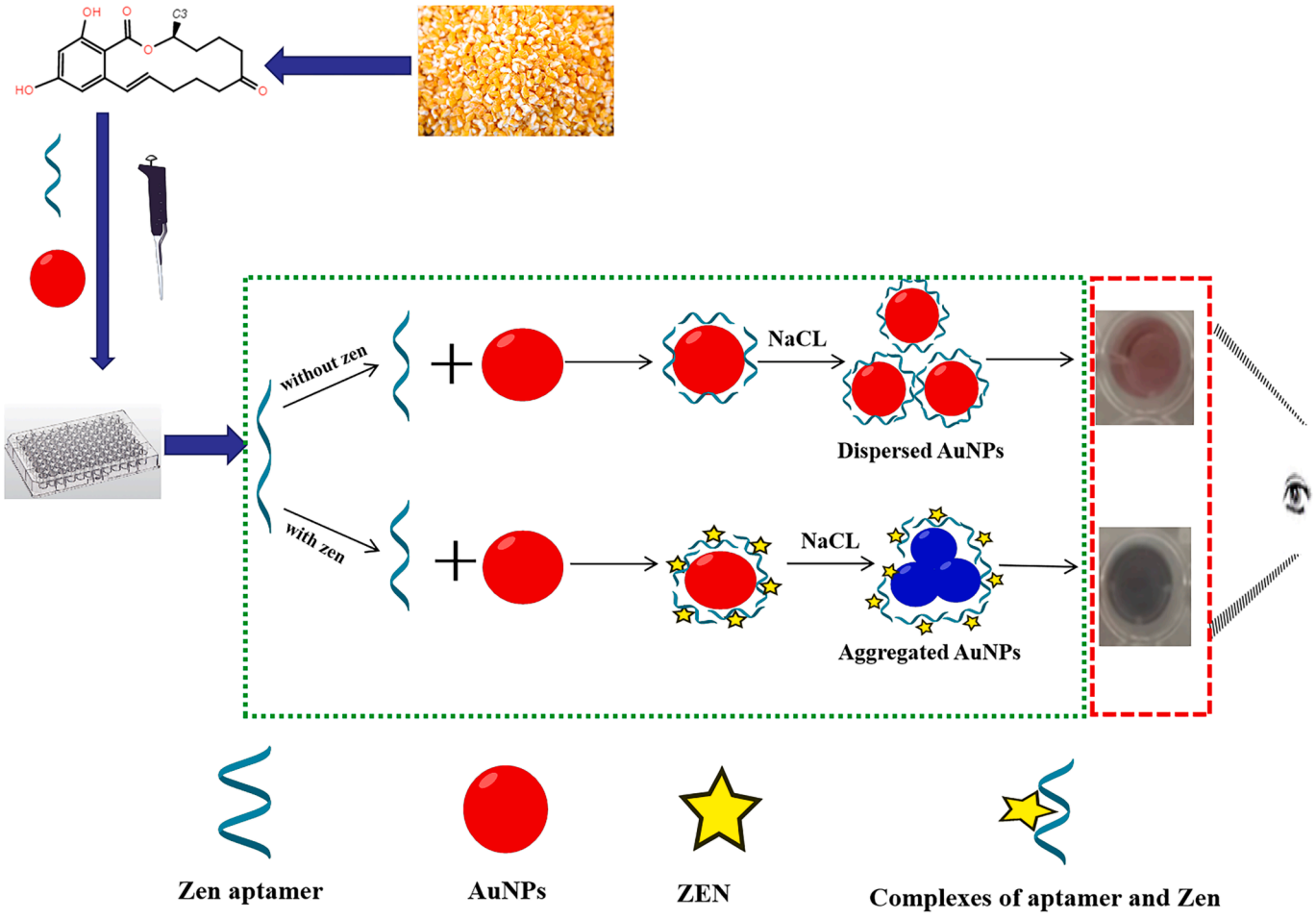

Fig. 1. Schematic diagram of the colorimetric aptamer sensor for ZEN detection. In the absence of ZEN, the color of the designed aptamer sensor is red. In the presence of ZEN, the color of the aptamer sensor is blue. (For interpretation of the references to color in this figure legend, the reader is referred to the web version of this article.)

3.2. Characterization of AuNPs

The prepared AuNPs solution was wine red in color, with uniform color distribution and no precipitation. As shown in Fig. 2 and Fig. 3, it could be seen that the prepared AuNPs solution had a single absorption peak at A520 nm, and no miscellaneous peak appeared. The result of transmission electron microscopy showed that the prepared AuNPs solution was relatively homogeneous and disperse. The prepared AuNPs had a uniform particle size (15 nm) and a uniformly dispersed spherical shape. The obtained experimental results were compared with the experimental results reported (Wu et al., 2019), and the results shown were similar to the patterns reported in the literature. It indicated that this method for preparing AuNPs could be used for subsequent experiments.

3.3. Optimization of experimental parameters

3.3.1. Optimization of NaCl concentration

Appropriate concentration of NaCl could reduce the background interference and improve the sensitivity of detection. However, in high concentration of salt, AuNPs will aggregate and their color would change from wine red to blue. That is to say, the concentration of NaCl directly affected the degree of aggregation of AuNPs. As can be seen from Suppl. Fig. S1, AuNPs showed a peak value at A650 nm with the the increase of NaCl concentration, and the absorbance value at A650 nm also increased with the increase of NaCl concentration, whereas the peak value at A520 nm gradually decreases. Therefore, the absorbance value at A650 nm was selected to measure the aggregation degree of AuNPs in this experiment.

It can be seen from Suppl. Fig. S2 that AuNPs hardly aggregated in NaCl solution with a concentration of 0–1 mol/L, and the color was still stable red. The reason was that NaCl was used to neutralize the charge on the surface of AuNPs. The addition of a small amount of NaCl did not induce aggregation of AuNPs due to the insufficient charge neutralization on the surface of AuNPs. And the color of the solution did not change significantly. When the concentration of NaCl was 1.5–3 mol/L,

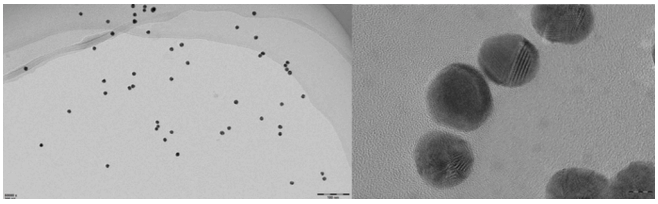

Fig. 3. Transmission electron microscope of AuNPs.

AuNPs solution began to aggregate. With the increase of NaCl concentration, the absorbance value of A650 nm increased continuously. When the concentration of NaCl reached 2 mol/L, the absorbance value of A650 nm tended to be stable. The ionic intensity increased with increasing NaCl concentration. The salt ions had a strong shielding effect on the negative charges on the surface of AuNPs. It shielded the electrostatic repulsion between the charges on the surface of AuNPs. Therefore, the gravitational force between adjacent AuNPs leaded to the aggregation of AuNPs when the NaCl concentration was further increased by 2 mol/L. The color of the solution turned blue. As can be seen from Suppl. Fig. S2, with the increase of NaCl concentration, the color and absorbance value of the solution no longer changed. This was because the AuNPs in the solution had sufficiently aggregated in the presence of NaCl (2 mol/L). Comparing the experimentally obtained results with those reported in the article by (Sun et al., 2020), the results were consistent with those reported in the literature. Therefore, the optimal concentration of NaCl addition was chosen to be 2 mol/L.

3.3.2. Optimization of aptamer concentration

Aptamers can protect AuNPs from agglomeration under high salt conditions to a certain extent, but it is not the case that the more the amount of aptamer is better. If there are too many aptamers, AuNPs will not agglomerate and change color in solutions with high salt concentration. This will not only affect the color change of the whole system, but also increase the cost. And a small amount of aptamer does not provide protection. So exploring the optimal concentration of aptamer

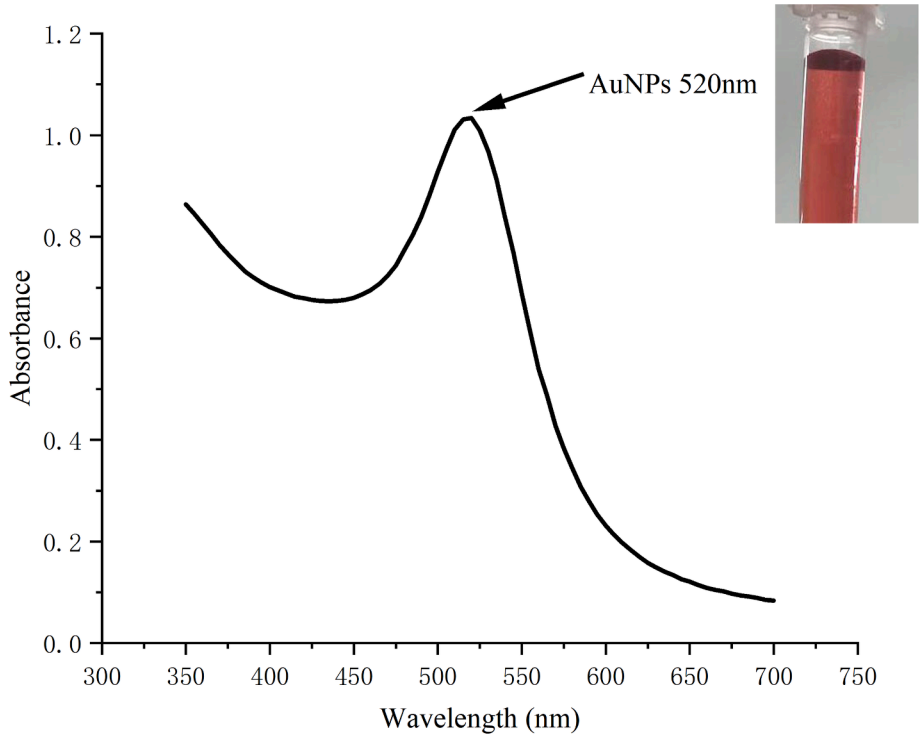

Fig. 2. UV–Vis absorption spectrum of AuNPs solution.

was crucial for the whole experiment. In order to determine the optimal concentration of aptamer we selected 0–9 umol/L aptamer as the optimized condition, respectively. The results are shown in Suppl. Fig. S3. When the aptamer concentration was 0–4 umol/L, the AuNPs were in the aggregated state. The color of the solution was blue and the absorbance value at A650 nm gradually increased. This was because with the increase of aptamer concentration, the surface of AuNPs adsorbed the aptamer on the surface of AuNPs due to electrostatic adsorption. However, the aptamer concentration was too low to prevent the NaCl induced AuNPs aggregation. Therefore, the AuNPs were still in the aggregation state, so the absorbance gradually increased. With the addition of aptamer to 5 umol/L, the absorbance of the solution at A650nm stabilized and the color of the solution was red. This was due to the saturation of the aptamer adsorbed on the surface of AuNPs with the increase of the aptamer concentration. The NaCl induced aggregation of AuNPs was prevented and the solution color changed to red. As the concentration of aptamer increased the aptamer on the surface of AuNPs was relatively more. And there was also free aptamer in the solution, which helped to maintain the stability between the aptamer and AuNPs in the solution. Therefore, the coalescence of AuNPs occurred to a lesser extent under the action of sodium chloride. Therefore, the color of the solution was red and the absorbance value at A650 nm tended to be stable. Comparing the experimental results with those reported by (Zhang et al., 2018), the results showed that the concentration of the aptamer required was greater than that reported in the literature. It was because the size of the prepared AuNPs was not the same. The size of AuNPs reported in the literature was 13 nm, while the one prepared in this work was 15 nm. Since the particle size of AuNPs was larger, a larger concentration of aptamer was needed to adsorb on the surface of prepared AuNPs and played a protective role. Therefore, the concentration of aptamer was 5 umol/L in experiments.

3.3.3. Optimization of incubation time of AuNPs and aptamer

As shown in Suppl. Fig. S4, the absorbance value of the solution increased and then decreased at A650 nm with the reaction time extending. When the incubation time was 0 min, the reaction between ZEN and the aptamer was not yet sufficient. The aptamer was still adsorbed on the surface of AuNPs, resulting in the inability of AuNPs to aggregate in the NaCl solution. The color of the solution was still red. Therefore, the change of absorbance value at A650 nm was relatively small. With the reaction time extending, the reaction degree of ZEN and aptamer increased, the absorbance value at A650 nm increased significantly, and the color of the solution was blue. The absorbance value reached the maximum when the incubation time was 5 min. This was due to the continuous competition of the aptamer on the surface of AuNPs and the loss of protection of AuNPs, resulting in the aggregation of AuNPs in NaCl solution and the blue color of the solution. When the incubation time was greater than 5 min (5–30 min), the absorbance value of the solution at A650 nm gradually decreased. And AuNPs kept precipitating out, and the color of the solution gradually became lighter. Comparing the experimental results with reported by (Sun et al., 2020), the results shown were similar to the reported in the literature. This may be related to the fact that some aptamers that were shed and not tightly bound to ZEN were re-adsorbed on the surface of AuNPs. This is because it would weaken the agglomeration effect of AuNPs when reacting with NaCl solution. So the optimal incubation time was selected as 5 min.

3.4. Specificity and stability

In order to verify whether the method could specifically identify ZEN, three toxins commonly found in cereal, DON, T-2, and AFB_1 were selected for the specificity measurement under optimal conditions. The concentration of toxin was 30 ng/mL. As shown in Fig. 4, only the solution of the system with the addition of ZEN changed from red to blue under the optimal conditions. The absorbance value at A650 nm was significantly higher than that of the other three toxins. This was due to the strong specificity of the ZEN aptamer used and the fact that an aptamer can only specifically recognize the toxin corresponding to it and not to the others. Only the ZEN toxin specifically recognized the ZEN aptamer on the surface of AuNPs and scrambled the aptamer from the surface of AuNPs first, resulting in the loss of protection of AuNPs by the aptamer exposed to the solution. When sodium chloride solution was added AuNPs lost protection and aggregation occured, the solution turned blue and the absorbance value at A650 nm increased significantly. In contrast, the addition of the other three toxins solutions could not specifically bind the ZEN aptamer. Nor could the aptamer be

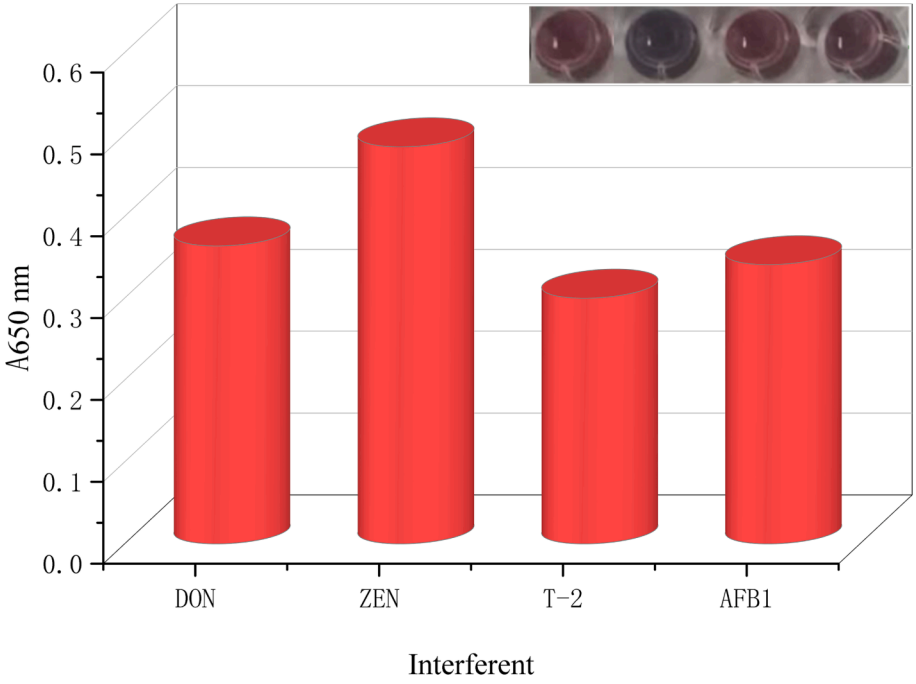

Fig. 4. Specificity of the proposed toxoid-a (atx-a) colorimetric aptamer sensor.

snatched from the surface of AuNPs. As a result, the AuNPs remained protected from inducing AuNPs aggregation when sodium chloride solution was added. This is manifested by the reaction solution remaining red and the absorbance value at A650 nm did not change. The experimental results were compared with those reported by (Sun et al., 2020). The results shown were similar to the pattern reported in the literature, with a clear change in the color and absorbance value of the solution. The results indicated that the specificity of the method was good.

To verify the stability of the constructed sensor, the sensor that was added with ZEN (30 ng/mL) was experimentally stored at refrigerated (4 ℃) and room temperature (25 ℃). And the test was performed every five days at the same time period (A650 nm) until the sensor response signal dropped to more than 15% of the initial value. As shown in Suppl. Fig. S5, the results showed that the sensor was maintained at 25 ℃ for only 10 days. However, the stability of the sensor could be maintained for 25 days at 4 ℃. This indicated that the sensor was more stable when stored at 4 ℃ and could be kept for up to nearly 4 weeks.

3.5. Linear range and detection limit of ZEN

Under the optimized experimental conditions, a series of different concentrations (0, 5, 50, 100, 150, 200, 250, 300, 350, and 400 ng/mL) of ZEN standard solution were assayed in order to plot the standard curve experiments. The linear equation was $Y = 0.0003\,X + 0.5128$, the linear range was 5–300 ng/mL, the correlation coefficient $R^2 = 0.9989$. The blank solution were carried out under optimized conditions, and the limit of detection the method was determined to be 5 ng/mL (S/N = 3).

3.6. Detection platform based on smartphone

In order to improve the convenience of the proposed method and facilitate detection outside the field or laboratory. In this work, a detection platform was constructed to read the color change of the detection system and analyze the RGB through a smartphone software in this work. As shown in Fig. 5, the reaction solution (AuNPs solution, NaCl, aptamer and sample solution) was added in the microplates. After 15 min of incubation of the reactants, the solutions in the different wells were firstly recorded by taking photos one by one using a smartphone quickly. Next, the RGB software in the smartphone was opened and the photos collected were uploaded to the software system one by one. In the next step, the software analyzed the ratio of "R", "G" and "B" to obtain a final RGB value from the ratio of the three. Finally, the concentration of ZEN was calculated according to the working curve.

As shown in Fig. 6(A and B), a series of photos were taken by a smartphone and these photos showed the color changes of ZEN concentration from 0 to 300 ng/mL. The color could be evaluated and converted to RGB values by the color recognizer app of the smartphone. The values of B/R (blue value/red value) in Fig. 6(C) showed good linear relationship in the concentration range of 5–300 ng/mL. The linear regression equation of ZEN was $y = 0.0006x + 1.0787$ ($R = 0.9975$).

3.7. Detection of actual samples

The maize samples and spiked samples containing ZEN (10, 50, and 100 ng/mL) were measured, and quantitative analysis was conducted. For purpose of optimizing experiments and reducing errors, all experiments must be performed in triplicate. The results are shown in Table 1. The recoveries ranges from 81.3 to 96.4 %, and the relative standard deviation (RSD) ranges from 1.0 to 5.7%. The ZEN in samples were undetectable. In this experiment, the national standard method and the method established in this work were used for the determination of maize, respectively. The paired T-Test was used to evaluate the consistency of the determination results of the two methods. As shown in Suppl. Table S2, the T-Test showed that the *t*-value was 0.121, Sig >0.05. Then, it indicated that there was no significant difference between the two methods.

3.8. Comparison of different methods

Compared with the reported detection methods (Sun et al., 2018; Kafouris et al., 2017; Li et al., 2021; Wu et al., 2018b) (Table 2), the proposed method has the advantages of low cost, visual, low detection limit and wide linear range, easy preparation of nanoparticles, does not need expensive instruments, convenient operation. Meanwhile, the proposed method can be used for more convenient and fast onsite analysis with the aid of smartphone, and the operation is simple, which also has certain practical application value.

4. Conclusion

The ZEN aptamer was used as the recognition element and AuNPs as the indicator. This work constructed a simple, fast, visualized, wide linear range, smartphone assisted colorimetric aptamer sensor. It could realize the visual measurement of zearalenone in maize by measuring absorbance values and visual observation of AuNPs color change. Compared with the current detection methods of ZEN, the developed aptasensor has several advantages. Firstly, in the presence of ZEN, the reaction solution changes from red to blue, which is visible to the naked eye, and is detected by absorbance values, which allows for easy detection of the cereals. Secondly, the whole process is completed within 15 min, achieving a fast detection capability. Thirdly, the reagents are complete and easy to prepare, reducing the cost of ZEN detection. The detection limit for ZEN was 5 ng/mL, with a linear range of 5–300 ng/mL, the recoveries ranged from 81.3 to 96.4%, and the method was used for the determination of ZEN in maize samples. The method was specific for the detection of ZEN. Overall the smartphone assisted colorimetric aptasensor can be applied to the ZEN detection of cereal samples.

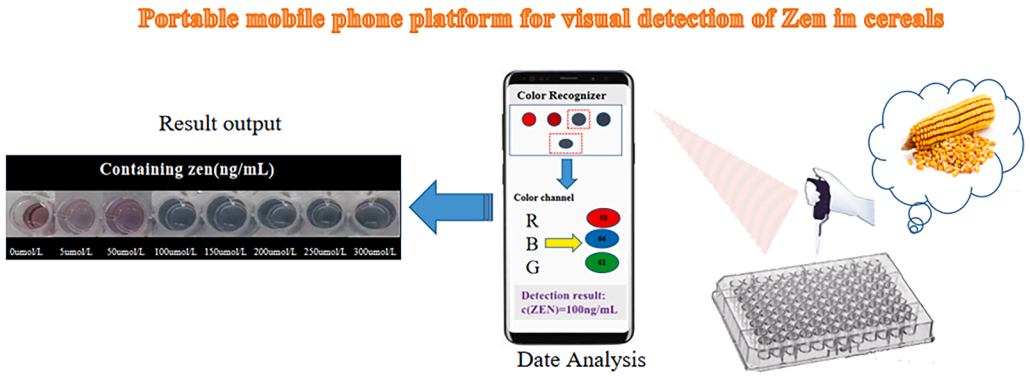

Fig. 5. Visual detection of ZEN in maize.

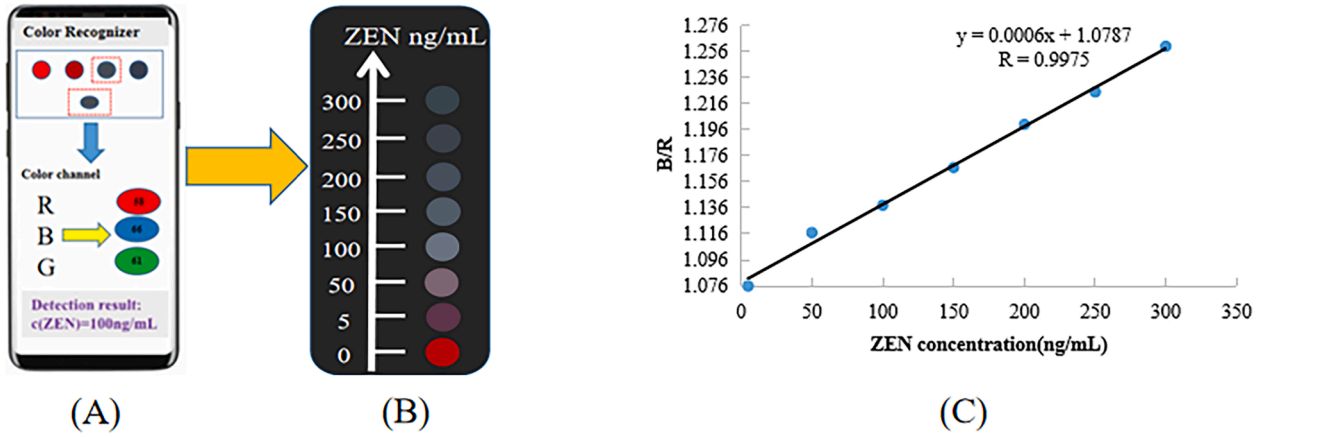

Fig. 6. (A) Schematic diagram of Zen detected by smart phone color recognizer. (B) ZEN(0–300 ng/mL)color change. (C) Linear diagram of color change (B/R of colorimetric aptasensor solution and ZEN concentration).

Table 1
Analytical results of maize sample.

Samples	Added of ZEN (ng/mL)	Recovery (%)	RSD (%)
Maize	10.00	81.3±5.69b	5.7
	50.00	93.5±1.15a	1.0
	100.00	96.4±2.35a	4.1

Table 2
Comparison of present method with other methods.

Matrix	Method	The linear dynamic range	LOD	Reference
Maize	Colorimetric aptasensor	5–300 ng/mL	5 ng/mL	This work
	Ultra performance liquid chromatography –Mass	5–640 μg/kg	3.1 μg/kg	Kafouris et al., 2017
	Aptamer-based lateral flow test strip	5–200 ng/mL	20 ng/mL	Wu et al., 2018
	Colorimetric assay based on Aptamer and AuNPs with peroxidase-like activity	10–250 ng/mL	10 ng/mL	2018
	A fluorescence resonance energy transfer probe based on functionalized graphene oxide and upconversion nanoparticles	0.005–100 ng/mL	0.0018 ng/mL	Li et al., 2021

CRediT authorship contribution statement

Liyuan Zhang: Methodology, Investigation. **Jiayu Chen:** . **Lifeng Lu:** . **Runzhong Yu:** Data curation, Formal analysis. **Dongjie Zhang:** Resources, Validation.

Declaration of Competing Interest

The authors declare that they have no known competing financial interests or personal relationships that could have appeared to influence the work reported in this paper.

Data availability

Data will be made available on request.

Funding

This work was supported by the Central Government for the Reform and Development of Local Universities in Heilongjiang Province [2020YQ16], the key research and development program guidance project of Heilongjiang province [GZ20210071].

Appendix A. Supplementary data

Supplementary data to this article can be found online at https://doi.org/10.1016/j.fochx.2023.100792.

References

Aiko, V., & Meht, A. (2015). Occurrence, detection and detoxification of mycotoxins. *Journal of Biosciences, 40*(5), 943–954. https://doi.org/10.1007/s12038-015-9569-6

Appel, M., & Bosma, W. B. (2011). Effect of surfactants on the spectrofluorimetric properties of zearalenone. *Journal of Luminescence, 131*(11), 2330–2334. https://doi.org/10.1016/j.jlumin.2011.05.061

Blokland, M. H., Sterkm, S. S., Stephany, R. W., Launay, F. M., Kennedy, D. G., & VanGinkel, L. A. (2006). Determination of resorcylic acid lactones in biological samples by GC-MS. Discrimination between illegal use and contamination with Fusariumtoxins. *Analytical Bioanalytical Chemistry, 384*, 1221–1227. https://doi.org/10.1007/s00216-005-0274-4

Chauhan, R., Singh, J., Sachdev, T., Basu, T., & Malhotra, B. D. (2016). Recent advances in mycotoxins detection. *Biosensors & Bioelectronics, 81*, 532–545. https://doi.org/10.1016/j.bios.2016.03.004

Chryseis L.L., Anders C.A.J., Allen P.G., 2011. DNA ligand for aflatoxin and zearalenone. US, WO/2011/020198. https://www.freepatentsonline.com/.

Fernandez H., Arevalo F., Granero A.M., Robledo S.N., Díaz Nieto C.H., Riber W.I., Zon M.A. (2017). Electrochemical biosensors for the determination oftoxic substances related to food safety developed in South America: myco-toxins and herbicides. *Chemosensors. 5* (3). 23. 1-20. doi: 10.3390/chemosensors5030023.

GB5009-.209-2016. Determination of zearalenone in food: liquid chromatographic method.

Goud, K. Y., Hayat, A., Satyanarayana, M., Kumar, V. S., Catanante, G., Gobi, K. V., et al. (2017). Aptamer-based zearalenone assay based on the use of a fluorescein label and afunctional graphene oxide as a quencher. *Microchimica Acta, 184*(11), 4401–4408. https://doi.org/10.1007/s00604-017-2487-6

Goud, K. Y., Kailasa, S. K., Kumar, V., Tsang, Y. F., Lee, S. E., Gobi, K. V., et al. (2018). Progress on nanostructured electrochemical sensors and their recognitionelements for detection of mycotoxins: A review. *Biosensors and Bioelectronics, 121*(15), 205–222. https://doi.org/10.1016/j.bios.2018.08.029

Ji, F., He, D., Olaniran, A. O., Mokoena, M. P., Xu, J. X., & Shi, J. R. (2019). Occurrence, toxicity, production and detection of Fusarium mycotoxin: A review. *Food Production, Processing and Nutrition, 1*, 6. https://doi.org/10.1186/s43014-019-0007-2

Kafouris, D., Christofidou, M., Christodoulou, M., Christou, E., & Kakouri, E. (2017). A validated UPLC-MS/MS multi-mycotoxin method for nuts and cereals: Results of the official control in Cyprus within the EU requirements. *Food and Agricultural Immunology, 28*(1), 90–108. https://doi.org/10.1080/09540105.2016.1228834

Kovalsky, P., Kos, G., Nährer, K., Schwab, C., Jenkins, T., Schatzmayr, G., et al. (2016). Co-Occurrence of Regulated, Masked and Emerging Mycotoxins and Secondary Metabolites in Finished Feed and Maize-An Extensive Survey. *Toxins, 8*(12), 363. https://doi.org/10.3390/toxins8120363

Li, Y. H., Li, X. Y., Zhang, D., Tian, W. L., Shi, J. Y., Li, Z. H., et al. (2021). A fluorescence resonance energy transfer probe based on functionalized graphene oxide and upconversion nanoparticles for sensitive and rapid detection of zearalenone. *LWT. Food Science and Technology, 147*, Article 111541. https://doi.org/10.1016/j.lwt.2021.11154

Li, P. W., Zhang, Z. W., Zhang, Q., Zhang, N., Zhang, W., Ding, X. X., et al. (2012). Current development of microfluidic immunosensing approaches for mycotoxin

detection via capillary electromigration and lateral flow technology. *Electrophoresis, 33*(15), 2253–2265. https://doi.org/10.1002/elps.201200050

Liu, P., Liu, N., Wang, Y. X., Duan, X. H., & Yin, W. L. (2016). Application of peptide nucleic acid probe in rapid detection of microorganisms. *Journal of Food Safety and Quality, 7*(4), 1363–1368. https://doi.org/10.19812/j.cnki.jfsq11-5956/ts.2016.04.001

Liu, L. H., Zhou, X. H., & Shi, H. C. (2015). Portable optical aptasensor forrapid detection of mycotoxin with a reversible ligand-grafted bio-sensing surface. *Biosensors & Bioelectronics, 72*, 300–305. https://doi.org/10.1016/j.bios.2015.05.033

Malachová, A., Stránská, M., Václavíková, M., et al. (2018). Advanced LC–MS-based methods to study the cooccurrence and metabolization of multiple mycotoxins in cereals and cereal-based food. *Analytical and Bioanalytical Chemistry, 410*, 801–825. https://doi.org/10.1007/s00216-017-0750-7

Mally, A., Solferizzo, M., & Degen, G. H. (2016). Biomonitoring of themycotoxin zearalenone: Current state-of-the art and application to human exposure assessment. *Archives of Toxicology, 90*(6), 1281–1292. https://doi.org/10.1007/s00204-016-1704-0

Man, Y., Liang, G., Li, A., & Pan, L. G. (2017). Recent advances in mycotoxin determination for food monitoring via microchip. *Toxins, 9(10), 324*, 1–24. https://doi.org/10.3390/toxins9100324

Meneely, J. P., & Elliott, C. T. (2014). Rapid surface plasmon resonance immunoassays for the determination of mycotoxins in cereals and cereal-based food products. *World Mycotoxin Journal., 7*(4), 491–505. https://doi.org/10.3920/WMJ2013.1673

Nguyen, D. K., & Jang, C. H. (2020). Label-free liquid crystal-based biosensor for detection of As(III) ions using ssDNA as a recognition. 22. probe. *Microchemical Journal, 156*, Article 104834. https://doi.org/10.1016/j.microc.2020.104834

Nimjee, S. M., Rusconi, C. P., & Sullenger, B. A. (2005). Aptamers: An emerging class of therapeutics. *Annual Review of Medicine, 56*, 555–583. https://doi.org/10.1146/annurev.med.56.062904.144915

Purohit, B., Vernekar, P. R., Shett, N. P., & Chandra, P. (2020). Biosensor nanoengineering: Design, operation, and implementation for biomolecular analysis. *Sensors. International, 1*, Article 100040. https://doi.org/10.1016/j.sintl.2020.100040

Ropejko, K., & Twaruzek, M. (2021). Zearalenone and Its Metabolites-General Overview. *Occurrence, and Toxicity, Toxins, 13*(1), 35. https://doi.org/10.3390/toxins13010035

Sharma, R., Ragavan, K. V., Thakur, M. S., & Raghavarao, K. S. M. S. (2015). Recent advances in nanoparticle based aptasensors for food contaminants. *Biosensors & Bioelectronics, 74*, 612–627. https://doi.org/10.1016/j.bios.2015.07.017

Solís-Cruz, B., Hernandez-Patlan, D., Beyssac, E., Latorre, J. D., Hernandez-Velasco, X., Merino-Guzman, R., et al. (2017). Evaluation of chi-tosan and cellulosic polymers as binding adsorbent materials to preventaflatoxin b1, fumonisin b1, ochratoxin, trichothecene, deoxynivalenol, and zearalenone mycotoxicoses through an in vitro gastrointestinal model for poultry. *Polymers, 9*(10), 529. https://doi.org/10.3390/polym9100529

Sun S.h., Zhao R., Feng S., Xie L.Y. (2018). Colorimetric zearalenone assay based on the use of an aptamer and of gold nanoparticles with peroxidase-like activity. *Microchim Acta.* 185. 535. doi: 10.1007/s00604-018-3078-x.

Sun, S. M., Ma, W. B., Wei, M., Li, Q., Xie, Y., & L.. (2020). Amplification based on aptamer nano gold silver staining Study on rapid detection method of Zearalenone. *Science and Technology of Cereals, Oils and Foods*. https://doi.org/10.16210/j.cnki.1007-7561.2020.05.003

Taghdisi, S. M., Danesh, N. M., Ramezani, M., Sarreshtehdar, A. E., & Abnous, K. (2018). A novel colorimetric aptasensor for zearalenonedetection based on nontarget-induced aptamer walker, gold nano-particles and exonuclease-assisted recycling amplification. *ACS Applied Mater Interfaces, 10*(15), 12504–12509. https://doi.org/10.1021/acsami.8b02349

Vasilescu, A., & Marty, J. L. (2017). Aptasensors, an analytical solutionfor mycotoxins detection. *Comprehensive Analytical Chemistry, 77*, 101–146. https://doi.org/10.1016/bs.coac.2017.05.006

Wu, S. J., Liu, L. H., Duan, N., Li, Q., Zhou, Y., & Wang, Z. P. (2018b). An aptamer-based lateral flow test strip for rapid detection of zearalenone in corn samples. *Journal of Agricultural and Food Chemistry, 66*(8), 1949–1954. https://doi.org/10.1021/acs.jafc.7b05326

Wu, Y. Y., Liu, B. W., Huang, P. C., & Wu, Y. F. (2019). A novel colorimetric aptasensor for detection of chloramphenicol based on lanthanum ion–assisted gold nanoparticle aggregation and smartphone imaging. *Analytical and Bioanalytical Chemistry, 411*, 7511–7518. https://doi.org/10.1007/s00216-019-02149-7

Wu, H., Liu, R., Kang, X. J., Liang, C. Y., Lv, L., & Guo, Z. (2018a). Fluorometricaptamer assay for ochratoxin A based on the use of single walledcarbon nanohorns and exonuclease III-aided amplification. *Microchimica Acta, 185*, 27. https://doi.org/10.1007/s00604-017-2592-6

Zhang, Y. Y., Lu, T. F., Wang, Y., Diao, C. X., Zhou, Y., Zhao, L. L., et al. (2018). Selection of a DNA Aptamer against Zearalenone and Docking Analysis for Highly Sensitive Rapid Visual Detection with Label-Free Aptasensor. *Journal of Agricultural and Food Chemistry, 66*(45), 12102–12110. https://doi.org/10.1021/acs.jafc.8b03963

Zhao, D. T., Gao, Y. J., Zhang, W. J., Bi, T. C., Wang, X., Ma, C. X., et al. (2021). Development a multi-immunoaffinity column LC-MS-MS method forcomprehensive investigation of mycotoxins contamination and co-occurrence in traditional Chinese medicinal materials. *Journal of Chromatography B, 15*, 1178. https://doi.org/10.1016/j.jchromb.2021.122730

Zheng, Y., Wang, Y., & Yang, X. R. (2011). Aptamer-based colorimetric biosensing of dopamine using unmodified gold nanoparticles. *Sensors and Actuators B: Chemical, 156*(1), 95–99. https://doi.org/10.1016/j.snb.2011.03.077

Zhu, L., Zhao, Y., Yao, S. C., Xu, M. Z., Yin, L. H., Zhai, X. H., et al. (2021). A colorimetric aptasensor for the simple and rapid detection of human papillomavirus type 16 L1 proteins. *Analyst, 146*, 2712–2717. https://doi.org/10.1039/d1an00251a